INSTITUTE OF PHYSICS PUBLISHING JOURNAL OF PHYSICS: CONDENSED MATTER

J. Phys.: Condens. Matter **14** (2002) 2547–2560 PII: S0953-8984(02)31143-3

Spectral properties of the Holstein double-exchange model and application to manganites

M Hohenadler[1] **and D M Edwards**

Department of Mathematics, Imperial College, London SW7 2BZ, UK

E-mail: d.edwards@ic.ac.uk

Received 22 November 2001, in final form 21 January 2002
Published 18 March 2002
Online at stacks.iop.org/JPhysCM/14/2547

Abstract

Calculations of one-electron spectral functions, optical conductivity and spin-wave energy in the Holstein double-exchange model are made using the many-body coherent potential approximation. Satisfactory agreement is obtained with angle-resolved photoemission results on $La_{1.2}Sr_{1.8}Mn_2O_7$ and optical measurements on $Nd_{0.7}Sr_{0.3}MnO_3$. A pseudogap in the one-electron spectrum at the Fermi level plays an important role in both systems, but a small-polaron band is only predicted to exist in the La system. A rigorous upper bound on spin-wave energies at $T = 0$ is derived. The spin-wave stiffness constant D decreases with increasing electron–phonon coupling g in a similar way to the Curie temperature T_C, but $D/(k_B T_C)$ increases for large g (low T_C) as observed experimentally.

1. Introduction

Recently there has been much interest in the manganite compounds $R_{1-x}A_xMnO_3$, where R is a rare-earth element such as La or Nd and A is a divalent metal ion such as Ca, Sr or Pb. These compounds are generally ferromagnetic for $x \simeq 0.2$–0.4 and in many of them, near the Curie temperature T_C, the electrical resistivity ρ decreases strongly in an applied magnetic field. This effect is known as colossal magnetoresistance (CMR) and a recent review is by Ramirez [1]. Ferromagnetism in these compounds is believed to be due to the 'double exchange' (DE) mechanism, which operates when local spins are strongly coupled, by Hund's rule, to the spins of itinerant electrons occupying a narrow band. The local spins, of magnitude $S = 3/2$, correspond to three localized Mn d electrons of t_{2g} symmetry and the band is derived from Mn d states of e_g symmetry. The band contains $n = 1 - x$ electrons/atom. Millis *et al* [2] stressed that to describe the physics of the manganites completely it is necessary to consider coupling of the electrons to local phonons as well as to local spins. Subsequently, Millis *et al* [3] made detailed calculations of such a model, with local spins and local moments

[1] Present address: Institut für Theoretische Physik, Technische Universität Graz, Graz A-8010, Austria.

treated classically, using dynamical mean field theory (DMFT). Recently Green [4], extending a many-body coherent potential approximation (CPA) developed by Edwards *et al* [5, 6] for the pure DE model, considered a similar model with local spins and phonons treated quantum mechanically. In the classical spin limit of the DE model the many-body CPA is equivalent to the DMFT of Furukawa [7, 8]. Green [4] discussed a number of physical properties of the model with electron–phonon coupling, which he called the Holstein-DE model. These include the resistivity, and its dependence on the applied magnetic field (the CMR effect) and on pressure, and the Curie temperature T_C. In section 2 we summarize the many-body CPA treatment of the Holstein-DE model and comment on the application of Green's results to the manganites. The aim of this paper is to calculate some spectral properties of the model and to compare with experimental results. We restrict our attention to the paramagnetic state and the ferromagnetic ground state where the many-body CPA simplifies considerably. In section 3 we calculate spectral functions which relate to the results of angle-resolved photoemission (ARPES) and in section 4 we consider the optical conductivity. In section 5 we calculate the spin-wave stiffness constant in the ferromagnetic state at $T = 0$ and show how it decreases with increasing electron–phonon coupling in a similar way to T_C. A brief summary is given in section 6.

2. Many-body CPA for the Holstein-DE model

The Hamiltonian of the Holstein-DE model in the absence of an applied magnetic field is

$$H = \sum_{ij\sigma} t_{ij} c^\dagger_{i\sigma} c_{j\sigma} - J \sum_i \boldsymbol{S}_i \cdot \boldsymbol{\sigma}_i - g \sum_i n_i (b^\dagger_i + b_i) + \omega \sum_i b^\dagger_i b_i. \tag{1}$$

The first two terms constitute the DE model and the first, third and fourth terms form the Holstein model [9]. Einstein phonons on site i, with energy ω and creation operator $b^\dagger_i$ couple to the electron occupation number $n_i = \sum_\sigma n_{i_\sigma}$ with coupling strength g. Here $n_{i\sigma} = c^\dagger_{i\sigma} c_{i\sigma}$, where $c^\dagger_{i\sigma}$ creates an electron of spin σ on lattice site i. The conduction electron spin $\boldsymbol{\sigma}_i = (\sigma_i^x, \sigma_i^y, \sigma_i^z)$ couples to the local spin $\boldsymbol{S}_i$ with Hund exchange parameter $J > 0$, and t_{ij} is the band hopping integral. The components of $\boldsymbol{\sigma}_i$ are defined as

$$\sigma_i^+ = \sigma_i^x + \mathrm{i}\sigma_i^y = c^\dagger_{i\uparrow} c_{i\downarrow}, \qquad \sigma_i^- = \sigma_i^x - \mathrm{i}\sigma_i^y = c^\dagger_{i\downarrow} c_{i\uparrow}, \qquad \sigma_i^z = \tfrac{1}{2}(n_{i\uparrow} - n_{i\downarrow}). \tag{2}$$

It is reasonable to assume that the manganites are in the DE limit $J \gtrsim W$ [10], where $2W$ is the width of the itinerant electron band, and in this paper we assume $J = \infty$. This ensures that there is no double occupation of a site by electrons, so that the system is a Mott insulator for $n = 1$. This is not so for the two-band model used by Millis *et al* [2], and Held and Vollhardt [11] have stressed the need to introduce a strong on-site Coulomb interaction in this case. Clearly the one-band model neglects effects of e_g orbital degeneracy such as a proper treatment of the Jahn–Teller effect and the orbital ordering which occurs in the undoped system ($n = 1$). However, the nature of the local phonon mode in equation (1) is not specified and could correspond to a tetrahedral distortion of the oxygen octahedron surrounding a Mn site as in the dynamical Jahn–Teller effect.

An important feature of the many-body CPA for the one-particle retarded Green function is that it becomes exact in the atomic limit $t_{ij} = 0$. In this limit, and with $J = \infty$, the Green function is given by [4]

$$G^{\mathrm{AL}}(\epsilon) = \sum_{r=-\infty}^{\infty} \frac{I_r\{2\lambda[b(\omega)(b(\omega)+1)]^{1/2}\}}{(2S+1)\exp\{\lambda[2b(\omega)+1]\}} \times \frac{(2S+1)^{\frac{n}{2}} \exp(r\beta\omega/2) + (S+1)(1-n)\exp(-r\beta\omega/2)}{\epsilon + r\omega}, \tag{3}$$

where I_r is the modified Bessel function, $\lambda = g^2/\omega^2$ and $b(\omega) = (\exp(\beta\omega) - 1)^{-1}$ is the Bose function with $\beta = (k_B T)^{-1}$. In taking the limit $J \to \infty$ we have made a shift of energy origin $\epsilon \to \epsilon - JS/2$ and the polaron binding energy $\lambda\omega$ is also absorbed in the chemical potential. The form of the many-body CPA used by Green [4] for finite band-width becomes particularly simple in the paramagnetic state. For a band density of states of elliptic form $D_e(\epsilon) = [2/(\pi W^2)]\sqrt{W^2 - \epsilon^2}$, the local Green function $G(\epsilon)$ satisfies the CPA equation

$$G(\epsilon) = G^{AL}(\epsilon - W^2 G/4). \tag{4}$$

Furthermore the self-energy $\Sigma(\epsilon)$ is related to the local Green function by the equation [5]

$$\Sigma(\epsilon) = \epsilon - G^{-1} - W^2 G/4. \tag{5}$$

As well as the paramagnetic state, we shall also consider the case of a completely saturated ferromagnetic state at zero temperature, with all local and itinerant spins aligned. Then the double-exchange term in equation (1) becomes merely a constant shift in energy and the Hamiltonian is equivalent to that of the pure Holstein model. Within the many-body CPA the saturated state is actually the self-consistent ground state only for $S = \infty$ [4] and we shall mainly consider this limit. It is found that in the DE model [5,6] neither T_C nor the resistivity vary enormously with S so that this is a reasonable approximation to the $S = 3/2$ Mn spin. In the saturated ferromagnetic state at $T = 0$, with all n electrons per atom having $\uparrow$ spin, the local Green function $G_\uparrow(\epsilon)$ again satisfies equation (4) with G^{AL} replaced by

$$G^{AL}_\uparrow(\epsilon) = e^{-\lambda}\left\{\frac{1}{\epsilon} + \sum_{r=1}^{\infty}\frac{\lambda^r}{r!}\left(\frac{n}{\epsilon + \omega r} + \frac{1-n}{\epsilon - \omega r}\right)\right\}. \tag{6}$$

The many body CPA is successful in describing the crossover from weak electron–phonon coupling, through intermediate coupling where small-polaron bands begin to appear, to strong coupling where some results similar to those of standard small-polaron theory are recovered. It therefore extends the work of Millis *et al* [3], where phonons are treated classically, to the quantum small-polaron regime. One important quantum effect on a thermodynamic property is the behaviour of T_C for strong electron–phonon coupling. Millis *et al* [3] find $T_C \sim g^{-4}$ whereas Green [4] finds T_C is exponentially small for $g/W \gtrsim 0.35$. The physics is dominated by a very narrow polaron band. Green [4] showed how the Holstein-DE model could describe the very different behaviour of $La_{1-x}Sr_xMnO_3$ (LSMO) and $La_{1-x}Ca_xMnO_3$ (LCMO), with $x \sim 0.33$ where T_C is largest. In LSMO the resistivity ρ increases monotonically with temperature T, with a metal–poor-metal transition at T_C, whereas LCMO shows a metal–insulator transition with ρ decreasing with T above T_C. Also $\rho(T_C)$ is an order of magnitude smaller in LSMO than in LCMO, This type of behaviour can be understood in the Holstein-DE model by assuming that g/W is about 50% larger in LCMO than in LSMO and, within the model, this is consistent with the considerably lower T_C in LCMO. (The form of $\rho(T)$ in figure 7 of [4] is indistinguishable for $g/W = 0.1$ from that shown for $g/W = 0.01$ [12] and contrasts strongly with the curve in figure 6 for $g/W = 0.16$.) The calculated resistivity is not as sensitive to applied magnetic field and pressure as observed but this discrepancy might be removed by introducing a decrease in g/W with decreasing resistivity owing to enhanced screening of the ionic charges [4]. A defect of the CPA treatment is its failure to describe coherent Bloch-like states in the saturated ferromagnetic state at $T = 0$, leading to a spurious residual resistivity [4].

In this paper we calculate further properties of the Holstein-DE model and confront them with experiment.

3. Angle-resolved photoemission spectroscopy (ARPES)

The decreasing resistivity of LCMO as the temperature increases above T_C is, according to Millis *et al* [3] and Green [4], due to the gradual filling of a pseudogap in the density of states. In Green's work the pseudogap contains well-defined polaron sub-bands in the (hypothetical) paramagnetic state at $T = 0$ but above T_C, with parameters appropriate to LCMO, these are smeared out so as to resemble the classical picture of Millis *et al*. The pseudogap should be observable in ARPES measurements and in optical conductivity. In an excellent paper on ARPES for the bilayer manganite $La_{1.2}Sr_{1.8}Mn_2O_7$, nominally with $n = 0.6$, Dessau *et al* [13] interpret their results very much in the spirit of the Holstein model. In this section we present some calculations of the spectral functions in the low-temperature ferromagnetic state to compare with this experimental data. For convenience we take $n = 0.5$ and also $S = J = \infty$, as discussed above. The charge ordering which might occur for $n = 0.5$ is suppressed since our treatment imposes spatial homogeneity. With this constraint there is no qualitative difference between systems with $n = 0.5$ and with 0.3 or 0.6, for example. We take the phonon energy to be $\omega/W = 0.05$, the same typical value used in previous calculations [4]. A half-width $W = 1$ eV is consistent with the e_g bands crossing the Fermi level in the calculations of Dessau *et al* [13], shown in figure 3(*b*). The low $T_C = 126$ K in this bilayer manganite is partly due to quasi-two-dimensional fluctuations, but the large resistivity $\rho \simeq 3$ mΩ cmat low temperatures indicates that small-polaron bands might exist even in the ferromagnetic state. Consequently the electron–phonon coupling should be stronger than in cubic manganites like LCMO and we choose $g/W = 0.2$.

The one-electron spectral function is given by

$$A_{\boldsymbol{k}}(\epsilon) = -\pi^{-1}\mathrm{Im}\,[\epsilon - \epsilon_{\boldsymbol{k}} - \Sigma(\epsilon)]^{-1} = -\pi^{-1}\Sigma''_\epsilon/[(\epsilon - \epsilon_{\boldsymbol{k}} - \Sigma'_\epsilon)^2 + \Sigma''^2_\epsilon] \tag{7}$$

where Σ'_ϵ, Σ''_ϵ are the real and imaginary parts of the self-energy $\Sigma(\epsilon)$ and $\epsilon_{\boldsymbol{k}}$ is the band energy for wavevector $\boldsymbol{k}$. In the ferromagnetic state at $T = 0$ the local Green function $G_\uparrow(\epsilon)$ is calculated from equation (4), with G^{AL} defined by (6), and $\Sigma(\epsilon)$ follows from equation (5). These equations assume an elliptic density of states which we here regard as an approximation to the density of states for a band which takes the form $\epsilon_{\boldsymbol{k}} = -W\cos\pi y$ for $\boldsymbol{k} = \pi(1, y)$, $0 \leqslant y \leqslant 1$. This band is shown as a full curve in figure 3(*a*) and crosses the Fermi level E_F at $\boldsymbol{k} = \pi(1, \frac{1}{2})$. It roughly models one of the $x^2 - y^2$ bands in figure 3(*b*). The calculated results for $A_{\boldsymbol{k}}$ are shown in figure 1. Well away from the Fermi level, a well-defined peak exists which broadens as $\boldsymbol{k}$ approaches the Fermi momentum at $y = 0.5$. For larger y the weight below the Fermi level is strongly reduced. The peaks never approach the Fermi level closely which is an important feature of the observed spectra [13] reproduced in figure 2. The theoretical curves in figure 1 resemble quite closely the data of figure 2(*c*). There is a pseudogap in the calculated spectra extending about 0.1 eV on each side of the Fermi level. In fact this pseudogap contains polaron bands like those shown in figure 4 of Green's paper [4]. However, their amplitude is too small to show up in figure 1 and in the experimental data. Nevertheless, it is the central polaron band around the Fermi level which is responsible for the low but finite conductivity of the system. The positions of the peaks in figure 1 are plotted in figure 3(*a*) and comparison can be made with the right half of figure 3(*b*) reproduced from Dessau *et al* [13]. Filled and unfilled symbols correspond to high and low weights, respectively, obtained by integration of the spectral function up to the Fermi energy. This comparison between theory and experiment supports the conclusion of Dessau *et al* [13] that, in the manganites with a layered structure, strong electron–phonon coupling (with the appearance of a pseudogap) is already important below T_C. This contrasts with the usual pseudocubic manganites where the pseudogap only appears above T_C. Previous work related to ours is the calculation by

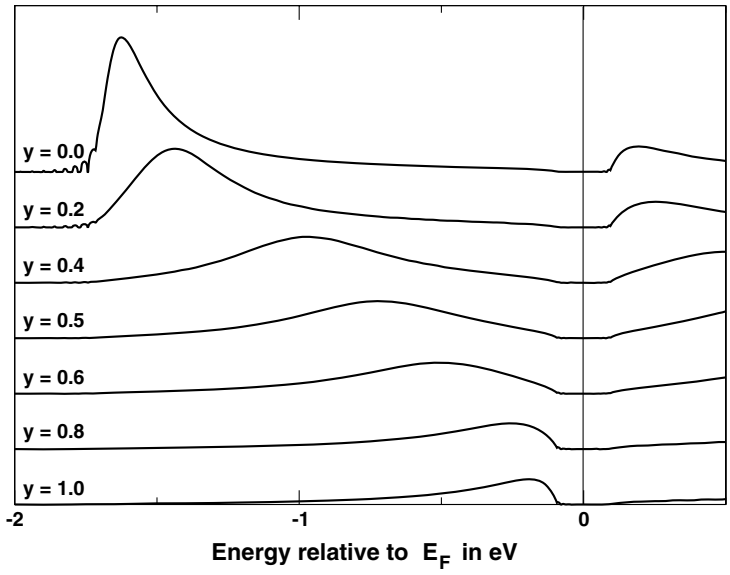

Figure 1. The spectral function $A_k(\epsilon)$ in the ferromagnetic state at $T = 0$ for $J = S = \infty$, $n = 0.5$ and strong electron–phonon coupling $g/W = 0.20$, with $\boldsymbol{k} = \pi(1, y)$.

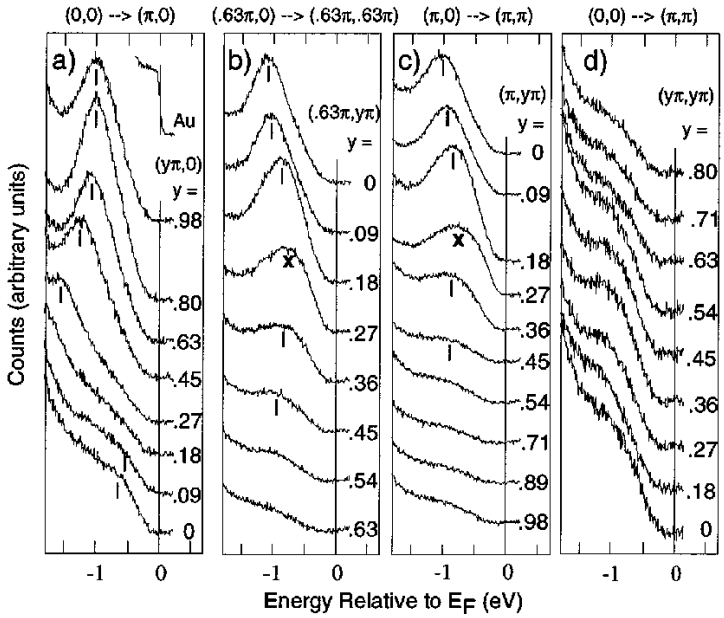

Figure 2. ARPES spectra of $La_{1.2}Sr_{1.8}Mn_2O_7$ ($T_C = 126$ K) in the ferromagnetic state at $T = 10$ K, reproduced from Dessau *et al* [13].

Perebeinos and Allen [14] of ARPES spectra in a two-band model of undoped $LaMnO_3$. It should be mentioned that Moreo *et al* [15] interpret the observed pseudogap not as an intrinsic property but in terms of phase separation.

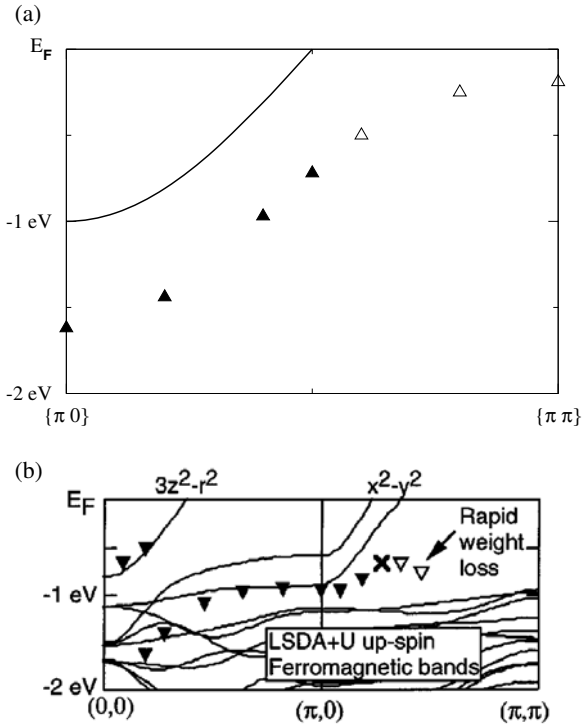

Figure 3. (*a*) The band energy ϵ_k (——) and the position of the peak centres in figure 1. Different symbols denote high (▲) and low (△) spectral weight, obtained by integration over the spectral function up to the Fermi energy E_F. (*b*) Virtual crystal LSDA + U majority spin bands for $La_{1.2}Sr_{1.8}Mn_2O_7$ with experimental peaks from figure 2, reproduced from [13].

4. Optical conductivity

In the local approximation of CPA or DMFT there is no vertex correction in the current–current response function which may thus be expressed in terms of the one-particle spectral function. In the paramagnetic state the optical conductivity is given by [5, 16]

$$\sigma(\nu) = \frac{2\pi e^2}{3Na^3\hbar} \sum_{\boldsymbol{k}} \boldsymbol{v}_{\boldsymbol{k}}^2 \int \mathrm{d}\epsilon A_{\boldsymbol{k}\sigma}(\epsilon) A_{\boldsymbol{k}\sigma}(\epsilon+\nu) \frac{f(\epsilon) - f(\epsilon+\nu)}{\nu}, \tag{8}$$

where the electron velocity $\boldsymbol{v}_{\boldsymbol{k}} = \nabla\epsilon_{\boldsymbol{k}}$, a^3 is the volume of the unit cell, $f(\epsilon) = \{\exp[\beta(\epsilon - \mu)] + 1\}^{-1}$ is the Fermi function and N is the number of lattice sites. Since $A_{\boldsymbol{k}}$ depends on $\boldsymbol{k}$ only through $\epsilon_{\boldsymbol{k}}$ we may define a function $\phi(\epsilon_{\boldsymbol{k}})$ such that $\phi'(\epsilon_{\boldsymbol{k}}) = A_{\boldsymbol{k}}(\epsilon) A_{\boldsymbol{k}}(\epsilon+\nu)$, where the dependence of ϕ on ϵ and ν has been suppressed in the notation. Hence the sum in equation (8) may be written as

$$\sum_{\boldsymbol{k}} \nabla\epsilon_{\boldsymbol{k}} \cdot \nabla\phi(\epsilon_{\boldsymbol{k}}) = -\sum_{\boldsymbol{k}} \phi(\epsilon_{\boldsymbol{k}}) \nabla^2\epsilon_{\boldsymbol{k}}, \tag{9}$$

the last step following by Gauss's theorem. For a simple cubic tight binding band $\epsilon_{\boldsymbol{k}} = -2t \sum_\alpha \cos k_\alpha a$, with α summed over x, y, z, $\nabla^2\epsilon_{\boldsymbol{k}} = -a^2\epsilon_{\boldsymbol{k}}$. Then the summand in equation (9) is a function of $\epsilon_{\boldsymbol{k}}$ only and equation (8) becomes

$$\sigma(\nu) = \frac{2\pi e^2}{3a\hbar} \int \mathrm{d}\epsilon \int \mathrm{d}E D_{\mathrm{c}}(E) E \phi(E) \frac{f(\epsilon) - f(\epsilon+\nu)}{\nu} \tag{10}$$

where $D_c(\epsilon)$ is the density of states for the simple cubic band. By using equation (7) in the definition of $\phi'(\epsilon_k)$, and integrating with respect to ϵ_k, we obtain

$$\phi = \frac{1}{\pi^2}\frac{1}{((\Sigma''_\epsilon - \Sigma''_{\epsilon+\nu})^2 + O^2)((\Sigma''_\epsilon + \Sigma''_{\epsilon+\nu})^2 + O^2)}\{\Sigma''_{\epsilon+\nu}(\Sigma''^2_{\epsilon+\nu} - \Sigma''^2_\epsilon + O^2)\arctan P + \Sigma''_\epsilon[(\Sigma''^2_\epsilon - \Sigma''^2_{\epsilon+\nu} + O^2)\arctan Q + \Sigma''_{\epsilon+\nu} O \log R]\}, \tag{11}$$

with

$$O = \Sigma'_\epsilon - \Sigma'_{\epsilon+\nu} + \nu, \qquad Q = \frac{\Sigma'_{\epsilon+\nu} - \nu - \epsilon + \epsilon_k}{\Sigma''_{\epsilon+\nu}},$$
$$P = \frac{\Sigma'_\epsilon - \epsilon + \epsilon_k}{\Sigma''_\epsilon}, \qquad R = \frac{\Sigma''^2_\epsilon + (\Sigma'_\epsilon - \epsilon + \epsilon_k)^2}{\Sigma''^2_{\epsilon+\nu} + (\Sigma'_{\epsilon+\nu} - \nu - \epsilon + \epsilon_k)^2}. \tag{12}$$

Since we calculate the self-energy Σ using the elliptic density of states $D_e(\epsilon)$, as discussed in section 2, it is reasonable to approximate $D_c(E)$ in equation (10) by $D_e(E)$. The integral over E can then be carried out by parts so that, using the definition of ϕ', we find

$$\sigma(\nu) = \frac{2\pi e^2}{3a\hbar}\int \mathrm{d}\epsilon \int \mathrm{d}E \frac{W^2 - E^2}{3} D_e(E) A_E(\epsilon) A_E(\epsilon + \nu)\frac{f(\epsilon) - f(\epsilon + \nu)}{\nu} \tag{13}$$

with $A_E(\epsilon)$ given by equation (7), ϵ_k being replaced by E. This is of the form given by Chung and Freericks [17] and Chattopadhyay *et al* [18]. If $D_c(E)$ in equation (10) is replaced by a Gaussian, corresponding to a hypercubic lattice in infinite dimensions, the factor $(W^2 - E^2)/3$ in equation (13) is replaced by a constant [5, 19]. In this paper we use equation (13) which is consistent with our previous calculations of $\sigma(0)$ [4, 5]. This expression satisfies the correct one-band sum rule [18,20] that $(2/\pi)\int_0^\infty \sigma(\nu)\,\mathrm{d}\nu = -Ke^2/(3a\hbar)$, where the 'kinetic energy' K is the thermal average per lattice site of the first term in the Hamiltonian (1).

As in section 3 we take $J = S = \infty$, $W = 1$ eV, $\omega = 50$ meV and, as previously [4, 5], $a = 5$ Å, which is slightly larger than the Mn–Mn distance in perovskite manganites. It is again convenient to take $n = 0.5$ so that for $J = S = \infty$ the chemical potential μ is fixed at the centre of the occupied band for all temperatures, by symmetry. In the ferromagnetic state at $T = 0$ the spin-degeneracy factor 2 in equation (13) is omitted.

There have been numerous optical investigations of the manganites and the experimental data and their interpretation are varied. For photon energy $\nu > 3$ eV various peaks in the optical conductivity have been assigned to interband transitions between the Hund's rule split bands and to charge-transfer transitions between the O 2p and the Mn e_g bands. The latter do not appear in our one-band model and our assumption of $J = \infty$ eliminates the upper Hund's rule band. Our calculated $\sigma(\nu)$ is therefore only non-zero in the region $\nu < 2.5$ eV and in general exhibits one peak. We shall focus the discussion by considering one material, $Nd_{0.7}Sr_{0.3}MnO_3$ (NSMO), which has been investigated by at least two experimental groups. In the paramagnetic state above T_C there is one feature common to data on both thin films [20,21] and single crystals [22]. This is a broad peak at about 1.2 eV with a maximum conductivity $\sigma_{max} \approx 0.7 - 0.9$ (mΩ cm)$^{-1}$. However in NSMO films T_C, as deduced from the maximum in the resistivity $\rho(T)$, is larger in oxygen-annealed films ($T_C \approx 230$ K) than in an unannealed sample ($T_C \approx 180$ K) [20, 21]. In a NSMO single crystal, on the other hand, $\rho(T)$ is essentially the same ($T_C \approx 200$ K) in polished and annealed samples but the peak in the polished sample is shifted to $\nu \simeq 1$ eV with a reduced $\sigma_{max} \approx 0.3$ (mΩ cm)$^{-1}$. Since $\rho(T)$ and $\sigma(\nu)$ are quantitatively quite similar in NSMO and LCMO [20] we model NSMO with electron–phonon coupling $g/W = 0.16$, the same value as proposed by Green [4] for LCMO. The dc conductivity $\sigma(0)$ at $T = 10$ K is also very similar in annealed NSMO and LCMO films, 2.9 and 3.3 (mΩ cm)$^{-1}$respectively [20]. The value for NSMO agrees well with a

measured $\sigma(0)$ of 3.2 $(\mathrm{m}\Omega\ \mathrm{cm})^{-1}$at $T = 15$ K in a NSMO single crystal [22]. The above-mentioned defect of the present CPA treatment is associated with the absence of the sharp quasi-particle peak in the spectral function which should exist in the ferromagnetic state at $T = 0$. Consequently the Drude peak in $\sigma(\nu)$ at low frequency is also absent.

Using the parameters discussed above the Curie temperature of the model is about 230 K [4] and in figure 4(a) we plot the calculated optical conductivity for the ferromagnetic state at $T = 0$ and the paramagnetic state at $T = T_C$ and $1.5T_C$. The low dc conductivity of 0.11 $(\mathrm{m}\Omega\ \mathrm{cm})^{-1}$at $T = 0$ is due to the inadequate treatment of the coherent ground state in the CPA. Fortuitously the incoherent scattering introduced by the CPA seems to model quite well the low temperature incoherent scattering in the unannealed NSMO sample of Kaplan *et al* [21] which has a dc conductivity of about 0.15 $(\mathrm{m}\Omega\ \mathrm{cm})^{-1}$at $T = 15$ K. This optical data is reproduced in figure 4(b) for comparison with the calculated results of figure 4(a). In annealed NSMO films [20], and in single crystals [22], $\sigma(\nu)$ in the low-temperature ferromagnetic state continues to rise with decreasing ν down to much lower photon energy, and $\sigma(0) \approx 3$ $(\mathrm{m}\Omega\ \mathrm{cm})^{-1}$.

As pointed out above, $\sigma(\nu)$ is much less sample dependent in the paramagnetic state above T_C and a quantitative comparison with theory is meaningful. In figure 4(a) $\sigma_{\max} \approx 0.15$ $(\mathrm{m}\Omega\ \mathrm{cm})^{-1}$and it must be remembered that this curve is the contribution of optical transitions within the e_g band only. To compare with the data of figure 4(b) one should subtract the background due to other transitions which might leave an effective $\sigma_{\max} \approx 0.3$ $(\mathrm{m}\Omega\ \mathrm{cm})^{-1}$. Bearing in mind the simplicity of the one-band model, this order-of-magnitude agreement between theory and experiment is satisfactory. Our calculated results are quite similar to those of figure 7(d) in Millis *et al* [3]. Clearly, for the present intermediate electron–phonon coupling strength, their classical treatment of phonons is sufficient to obtain the essential features of the optical conductivity. The calculated peak in $\sigma(\nu)$ with $\nu \approx 1$ eV arises from $\boldsymbol{k}$-conserving transitions across the type of pseudogap discussed in section 3. During the process an electron moves from one site to a neighbouring one which was previously unoccupied. The electron motion is accompanied by a lattice distortion, of Jahn–Teller type, which corresponds to a displacement of the local phonon oscillator coordinate in the Holstein-DE model. When an electron enters (leaves) a site the final displaced (undisplaced) oscillator is generally in an excited state with typical excitation energy g^2/ω. This is the atomic-limit polaron binding energy and for the parameters assumed here is about 0.5 eV. Thus the peak in $\sigma(\nu)$ occurs at about twice the polaron binding energy just as in the standard small-polaron theory [23]. However for the present intermediate electron–phonon coupling $g/W = 0.16$ polaron bands near the Fermi level are largely washed out above T_C [4], so standard small-polaron theory is not expected to apply to $\sigma(\nu)$ for low photon energies. In fact an activation energy in the dc conductivity of 0.25 eV, half the polaron binding energy as predicted by small-polaron theory [23], is about a factor 4 larger than one deduced from Green's [4] numerical calculations. Green's calculation of the dc resistivity above T_C is in reasonable agreement with experiments on NSMO where an activation energy of about 0.08 eV is found [24]. Lee *et al* [22] quote an activation energy of about 0.15 eV and, with undue reliance on small-polaron theory, expect to have a peak in $\sigma(\nu)$ at about 0.6 eV. Although there is no sign of such a peak in their data they claim that their one broad peak near 1.2 eV should be interpreted in terms of a two-peak structure, one near 1.5 eV and the other below 1 eV. Our interpretation of the 1.2 eV peak in $\sigma(\nu)$ for $T > T_C$ is broadly in line with that of several other previous authors [3, 20, 21]. However we stress again that, for moderate electron–phonon coupling standard small-polaron theory does not hold at low photon energy, where only states around the Fermi level are involved, so no simple link between peak position and the activation energy of the dc conductivity can be made. Below T_C the peak in $\sigma(\nu)$ shifts to lower frequency as the pseudogap rapidly fills in. However, in our calculations this shift is held up due to spurious incoherent scattering in the

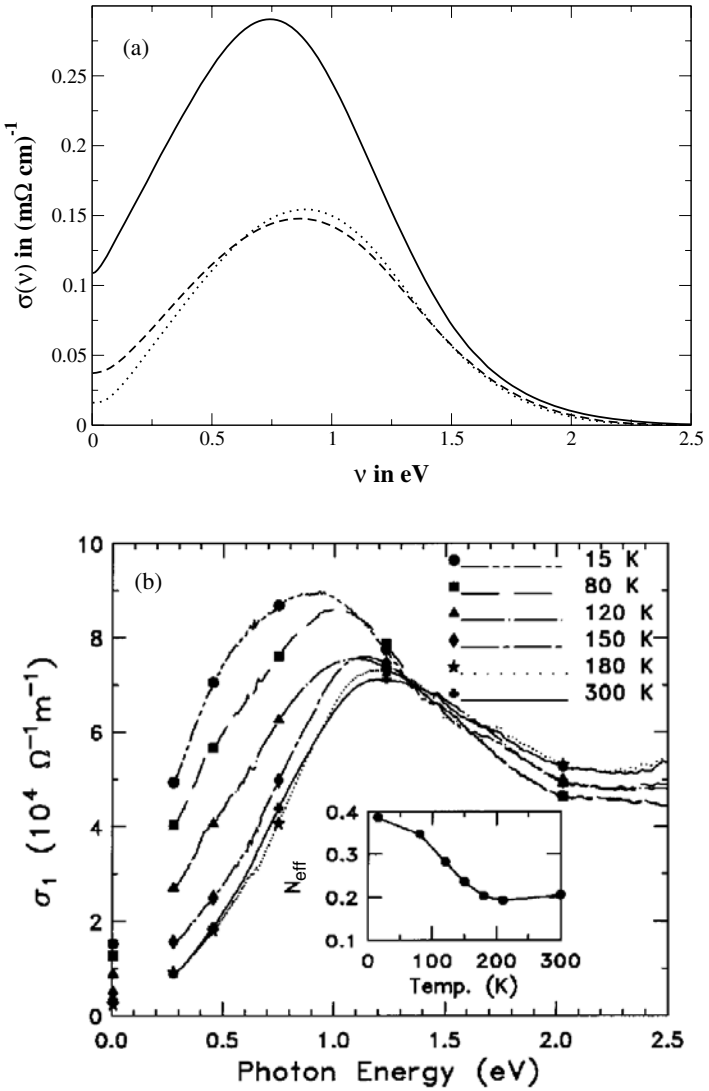

Figure 4. (*a*) Calculated optical conductivity for strong electron–phonon coupling $g/W = 0.16$ in the ferromagnetic state at $T = 0$ (——), the paramagnetic state at $T = T_C$ (· · · · · ·) and the paramagnetic state at $T = 1.5T_C$ (– – –). The plot is for $J = S = \infty$, $n = 0.5$ and $a = 5$Å. (*b*) Optical conductivity of $Nd_{0.7}Sr_{0.3}MnO_3$ at different temperatures, reproduced from Kaplan *et al* [21].

ground state, which limits the low-temperature dc conductivity. The same effect actually occurs in unannealed NSMO films (figure 4) but in annealed films and single crystals the peak shifts almost to zero frequency [20, 22]. The theoretical situation could be improved by introducing screening effects in the electron–phonon interaction so that g/W decreases with decreasing resistivity, as mentioned at the end of section 2. The spurious residual resistivity at $T = 0$ drops from 9 to 0.5 mΩ cmas g/W decreases from 0.16 to 0.10 [4, 12]. Ishihara *et al* [25] and Mack and Horsch [26] have given an alternative interpretation of the broad low-energy peak at $T = 0$ in terms of orbital degrees of freedom in the doubly degenerate e_g band. They propose

that strong correlation, with the constraint of no doubly occupied sites, leads to incoherent motion of the carriers.

5. The spin-wave spectrum

Quijada *et al* [20] considered the spin-wave stiffness constant D in the saturated ferromagnetic state at $T = 0$ and its relation to optical conductivity. However their derivation of an expression for D was restricted to the DE model. Here we derive a simple approximate formula for the spin-wave spectrum of the Holstein-DE model. Our main aim is to calculate D as a function of electron–phonon coupling strength and to compare with the corresponding behaviour of T_C. In the limit of $J \to \infty$ the local and itinerant spins are locked together as we make the ansatz

$$|q\rangle = (S_q^- + \sigma_q^-)\,|F\rangle \tag{14}$$

for the state (unnormalized as yet) with a magnon of wavevector $\boldsymbol{q}$ excited. Here $|F\rangle$ is the exact ferromagnetic ground state, which we assume to be one of complete spin alignment, and the spin lowering operators are defined by

$$S_q^- = \sum_i \mathrm{e}^{\mathrm{i}\boldsymbol{q}\cdot\boldsymbol{R}_i} S_i^-, \qquad \sigma_q^- = \sum_i \mathrm{e}^{\mathrm{i}\boldsymbol{q}\cdot\boldsymbol{R}_i} \sigma_i^-, \tag{15}$$

where $\boldsymbol{R}_i$ is the position of lattice site i.

Actually we do not know the state $|F\rangle$ exactly for the Holstein-DE model, unlike the DE model, but we shall only approximate it at a later stage. The spin-wave energy is given by

$$\omega_q = \frac{\langle q|\,H\,|q\rangle}{\langle q\,|\,q\rangle} - E_0 \tag{16}$$

where E_0 is the exact ground state energy, so that $H\,|F\rangle = E_0\,|F\rangle$. By the variational principle, this is an upper bound on ω_q. Using equation (14) it is easy to show that

$$\omega_q = \frac{\langle q|\,[H, S_q^- + \sigma_q^-]\,|F\rangle}{\langle q\,|\,q\rangle} \tag{17}$$

and $\langle q\,|\,q\rangle = N(2S+n)$, where S is the magnitude of the localized spin $\boldsymbol{S}_i$. Only the first term in the Hamiltonian (1) makes a non-zero contribution to the commutator. This one-electron term may be written as $\sum_{k\sigma} \epsilon_k n_{k\sigma}$ where $n_{k\sigma}$ is the occupation number for the Bloch state $\boldsymbol{k}\sigma$. A straightforward calculation yields

$$\omega_q = \frac{1}{N(n+2S)} \sum_{\boldsymbol{k}} (\epsilon_{k+q} - \epsilon_k)\langle n_{k\uparrow}\rangle \tag{18}$$

where $\langle n_{k\uparrow}\rangle = \langle F|n_{k\uparrow}\,|F\rangle$. Assuming a simple cubic tight-binding band $\epsilon_k = -t\sum_{\boldsymbol{R}} \mathrm{e}^{\mathrm{i}\boldsymbol{k}\cdot\boldsymbol{R}}$, the sum being over six nearest-neighbour sites, we find

$$\omega_q = -\frac{t}{N(n+2S)} \sum_{\boldsymbol{R}} (\mathrm{e}^{\mathrm{i}\boldsymbol{q}\cdot\boldsymbol{R}} - 1) \sum_{\boldsymbol{k}} \mathrm{e}^{\mathrm{i}\boldsymbol{k}\cdot\boldsymbol{R}} \langle n_{k\uparrow}\rangle. \tag{19}$$

Since $\langle n_{k\uparrow}\rangle$ has cubic symmetry in $\boldsymbol{k}$-space, the $\boldsymbol{k}$ sum in equation (19) is independent of the particular neighbour $\boldsymbol{R}$. By including the factor $-t$ it may therefore be written as $(1/6)\sum_{\boldsymbol{k}} \epsilon_k \langle n_{k\uparrow}\rangle$. Hence

$$\omega_q = \frac{D}{a^2} \sum_{\boldsymbol{R}} (1 - \mathrm{e}^{\mathrm{i}\boldsymbol{q}\cdot\boldsymbol{R}}) = (2D/a^2)(3 - \cos q_x a - \cos q_y a - \cos q_z a), \tag{20}$$

where $\boldsymbol{q} = (q_x, q_y, q_z)$ and

$$D = -\frac{a^2}{6N(n+2S)} \sum_{\boldsymbol{k}} \epsilon_k \langle n_{k\uparrow}\rangle = -\frac{Ka^2}{6(n+2S)}. \tag{21}$$

Here K is the expectation value of the kinetic energy which appears in the optical sum rule mentioned in section 4. By expanding equation (20) in powers of $\boldsymbol{q}$ to second order, we find $\omega_{\boldsymbol{q}} = Dq^2$ as that D defined by equation (21) is the spin-wave stiffness constant.

At this stage, with the expectation value $\langle n_{\boldsymbol{k}\uparrow}\rangle$ calculated in the exact ground state, equation (20) is a rigorous upper bound on the magnon energy for arbitrary J and S. This is no longer the case when we proceed to evaluate it within the many-body CPA. Clearly, equations (20) and (21) apply equally to the Holstein-DE and the DE model. However, we shall show that electron–phonon coupling in the former model has a strong influence via $\langle n_{\boldsymbol{k}\uparrow}\rangle$. In the limit $J \to \infty$, equation (21) is equivalent to results derived by Nagaev [27, 28], Kubo and Ohata [29], Furukawa [8, 30], Wang [31] and Quijada *et al* [20] for the DE model. The K defined in the latter paper is one-third of our kinetic energy. Furukawa also derived the dispersion relation of equation (20) for the DE model. Now

$$\langle n_{\boldsymbol{k}\uparrow}\rangle = \int_{-\infty}^{\mu} \mathrm{d}\epsilon A_{\boldsymbol{k}}(\epsilon) \tag{22}$$

where $A_{\boldsymbol{k}}(\epsilon)$, given by equation (7), is calculated for the saturated ferromagnetic state at $T = 0$. As in deriving $\sigma(\nu)$ we can replace the $\boldsymbol{k}$ sum in equation (21) by an energy integral. Hence, using the notation $A_E(\epsilon)$ introduced in equation (13),

$$D = -\frac{a^2}{6(n+2S)} \int_{-W}^{W} \mathrm{d}E \int_{-\infty}^{\mu} \mathrm{d}\epsilon E D_{\mathrm{e}}(E) A_E(\epsilon). \tag{23}$$

As in the previous section we have approximated the simple cubic density of states by the elliptic density of states $D_{\mathrm{e}}(E)$. To match the other calculations in this paper, in particular that of the optical conductivity, we calculate $A_E(\epsilon)$, and hence the double integral in equation (23) which represents the average kinetic energy K, in the limit $S = \infty$. However, in the prefactor in equation (23) we put $S = 3/2$ as is appropriate for the localized Mn spins. This corresponds to calculating the Bloch wall stiffness constant ($\propto D(n + 2S)$), which is a static quantity, in the limit $S \to \infty$ but retaining the essential finiteness of the spin in the dynamical quantity D. Otherwise we use the same parameters as in previous sections, except that we now take $a = 4$ Å. In section 4 we used $a = 5$ Å, for consistency with our earlier work on conductivity, but 4 Å is closer to the Mn–Mn distance in the pseudocubic manganites.

In figure 5 we plot the spin-wave stiffness D at $T = 0$ as a function of electron–phonon coupling g/W. The reason for the striking decrease of D with g/W, particularly in the range $0.1 < g/W < 0.2$ applicable to the manganites, is clear from equation (21). For $g/W = 0$, the pure DE model, $\langle n_{\boldsymbol{k}\uparrow}\rangle = 1$ for $\boldsymbol{k}$ within the Fermi surface and $\langle n_{\boldsymbol{k}\uparrow}\rangle = 0$ otherwise. The negative quantity K is the full non-interacting one-electron energy of the ferromagnetic state which drives the double-exchange mechanism. For larger g/W, $\langle n_{\boldsymbol{k}\uparrow}\rangle$ is more spread out over the whole zone and $|K|$ decreases. In an extreme limit where electrons are localized at sites, $\langle n_{\boldsymbol{k}\uparrow}\rangle$ is constant throughout the zone and hence $D = 0$. This behaviour of D in the Holstein-DE model is very similar to that of T_{C}, as calculated by Green [4]. The main difference is in the extreme strong-coupling limit where T_{C} becomes very small at $g/W \approx 0.35$ whereas D is decreasing quite slowly. The slow decrease of D is exactly what one expects from equation (21) and small-polaron theory, where the kinetic energy $K \sim g^{-2}$ [32]. T_{C} seems to be determined more by the width of the narrow polaron band around the Fermi level, which decreases exponentially with g. Thus one may expect that $D/(k_{\mathrm{B}}T_{\mathrm{C}})$ increases with increasing g, and thus with decreasing T_{C}. This is found experimentally, as discussed later.

Green and Edwards [6] find that, in the DE model with $n = 0.5$, T_{C} only increases by 5% when S increases from 3/2 to ∞. A similar insensitivity to S for $S \geqslant 3/2$ is expected in the Holstein-DE model. Hence, from equation (23), with $A_E(\epsilon)$ taken in the $S \to \infty$ limit as discussed, we have $\delta = D/(k_{\mathrm{B}}T_{\mathrm{C}}a^2) \propto (S + \frac{1}{2}n)^{-1}$. This is similar to the result $\delta = \frac{1}{2}(s+1)^{-1}$

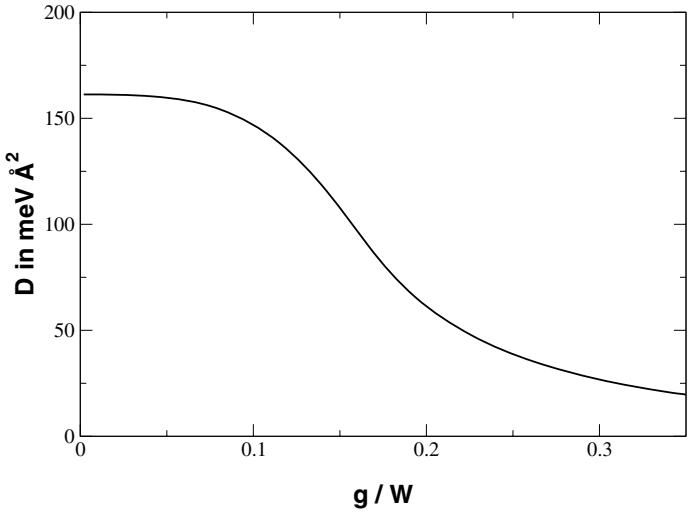

Figure 5. The spin-wave stiffness D versus electron–phonon coupling g in the saturated ferromagnetic state at $T = 0$. The plot is for $S = J = \infty$, $W = 1$ eV, $n = 0.5$ and $a = 4$ Å.

for the spin s nearest neighbour simple cubic Heisenberg model, with T_C calculated in mean field theory. Using values of T_C accurate to within about 1% [34] we find an improved Heisenberg value of $\delta = 0.286$ for $s = 3/2$, and $\delta = 0.258$ for an interpolated $s = 1.75$ which models the spin per site $S + \frac{1}{2}n$ in the present model. In the present calculations for D/a^2, together with those of Green [4] for T_C, we find, for $S = 3/2$, $\delta \approx 0.24$ for $g/W = 0.1$ and $\delta \approx 0.29$ for $g/W = 0.16$. With $a = 4$ Å these values correspond to $D/(k_B T_C) \approx 3.9$ and 4.6 Å^2, respectively. The agreement of these values of δ with the Heisenberg model suggests that for moderate g/W the ferromagnetic transition in the many-body CPA treatment of the Holstein-DE model is quite Heisenberg-like. However, this may not be the case for larger g/W where, as discussed above, δ increases rapidly with g/W.

To compare our theoretical results with experiment we first note that the simple spin-wave dispersion in equation (20), which is of the Heisenberg form, has been found to fit data on $La_{0.7}Pb_{0.3}MnO_3$ ($T_C = 355$ K) throughout the Brillouin zone [35]. In this work the low-temperature stiffness constant $D = 134$ meV Å^2 so that $D/(k_B T_C) = 4.4$ Å^2. In LSMO, also with $x = 0.3$, Martin *et al* [33] find $T_C = 378$ K and $D \approx 188$ meV Å^2 (at 27 K) so that $D/(k_B T_C) = 5.8$ Å^2. $Pr_{0.63}Sr_{0.37}MnO_3$ seems to behave similarly with $T_C = 301$ K, $D = 165$ meVÅ^2, $D/(k_B T_C) = 6.4$ Å^2 [36]. Although $D/(k_B T_C)$ in the last two materials is larger than in a Heisenberg model, their spin dynamics near T_C is quite conventional [33, 36]. However in some systems with lower T_C this is not the case, and $D/(k_B T_C)$ is considerably larger. Thus in LCMO, with $T_C = 250$ K, $D = 170$ meVÅ^2, $D/(k_B T_C) = 7.9$ Å^2, the ferromagnetic transition seems not to be a standard second-order one [37]. Also in NSMO, with $T_C = 198$ K, $D = 165$ meVÅ^2, $D/(k_B T_C) = 9.7$ Å^2, the spin-wave stiffness constant does not collapse to zero at $T = T_C$ [36], just as in LCMO [37]. It is not clear whether such behaviour could occur within the Holstein-DE model or whether inhomogeneity due to disorder is important. However, the larger values of $D/(k_B T_C)$ predicted by the model for strong electron–phonon coupling suggests that something unusual is going on. It is worth mentioning that D may be underestimated by the many-body CPA for an intermediate electron–phonon coupling such as $g/W = 0.16$ appropriate to LCMO. This is

because spurious incoherent scattering near the Fermi level reduces the 'kinetic energy' K, and hence D. On the other hand equation (21) itself gives an upper bound to D which, in a better approximation will certainly be reduced. For the DE model, in approximations equivalent to the random phase approximation (RPA) [20, 30, 31], this is achieved by an additional negative term proportional to Δ^{-1} where $\Delta = JS$ is the Hartree–Fock exchange splitting between up and down spin bands. In the presence of an onsite Coulomb interaction U, $\Delta = JS + Un$ so that the negative term is considerably reduced. RPA estimates of D in a two-band model differ widely [20, 38]. For the one-band model with $J = \infty$ and $S = 3/2$ Golosov [39] has shown that D is reduced to about half its $S = \infty$ value, over a wide range of band-filling, when magnon–electron scattering processes are considered. Further work on D in the Holstein-DE model is highly desirable.

6. Conclusion

The many-body CPA treatment of the Holstein-DE model has been used to investigate several spectral properties which may be compared with experimental data on the manganites. We have been able to supply the theory which was hinted at by Dessau *et al* [13] in the discussion of their ARPES measurements on the layered manganite $La_{1.2}Sr_{1.8}Mn_2O_7$ in the low-temperature ferromagnetic state. Broad spectral peaks lie either side of a pseudogap at the Fermi level and the pseudogap contains polaron subbands with exponentially small weight. One of these, at the Fermi level, is responsible for the poor metallic behaviour. We therefore agree with Alexandrov and Bratkovsky [40] that in this system, with unusually strong electron–phonon coupling, small polarons exist in the ferromagnetic state. However, we find that small-polaron theory does not apply above or below T_C in a pseudocubic manganite like $Nd_{0.7}Sr_{0.3}MnO_3$ with intermediate coupling strength. In particular the small-polaron result that the activation energy of the high-temperature dc conductivity is one-quarter of the peak photon energy in optical conductivity $\sigma(\nu)$ is found not to hold, in agreement with experiments on NSMO. The observed shift in spectral weight of $\sigma(\nu)$ to lower energy on going into the ferromagnetic state is found to occur, although it is somewhat suppressed by spurious incoherent scattering at $T = 0$ which is a defect of the theory. A rigorous upper bound is derived for spin-wave energies at $T = 0$ in the Holstein-DE model. It is shown that the spin-wave stiffness constant D decreases with increasing electron–phonon coupling strength in a similar way to T_C. However, for strong coupling the ratio $D/(k_B T_C)$ increases quite rapidly with increasing coupling strength, i.e. with decreasing T_C. This trend is found experimentally.

Acknowledgments

We thank Lesley Cohen and Dietrich Meyer for helpful discussion, and Jim Freericks for stimulating correspondence. One of us (MH) is grateful to the International Association for the Exchange of Students for Technical Experience (IAESTE), the Industriellenvereiningung Steiermark and Technical University Graz for financial support during a visit to Imperial College.

References

[1] Ramirez A P 1997 *J. Phys.: Condens. Matter* **9** 8171
[2] Millis A J, Littlewood P B and Shraiman B I 1995 *Phys. Rev. Lett.* **74** 5144
[3] Millis A J, Müller R and Shraiman B I 1996 *Phys. Rev.* B **54** 5405
[4] Green A C M 2001 *Phys. Rev.* B **63** 205110
[5] Edwards D M, Green A C M and Kubo K 1999 *J. Phys.: Condens. Matter* **11** 2791

[6] Green A C M and Edwards D M 1999 *J. Phys.: Condens. Matter* **11** 10 511
Green A C M and Edwards D M 2000 *J. Phys.: Condens. Matter* **12** 9107 (erratum)
[7] Furukawa N 1994 *J. Phys. Soc. Japan* **63** 3214
[8] Furukawa N 1996 *J. Phys. Soc. Japan* **65** 1174
[9] Holstein T 1959 *Ann. Phys., NY* **8** 343
[10] Sarma D D *et al* 1996 *Phys. Rev.* B **53** 6873
[11] Held K and Vollhardt D 2000 *Phys. Rev. Lett.* **84** 5168
[12] Green A C M, unpublished
[13] Dessau D S, Saitoh T, Park C-H, Shen Z-X, Villella P, Hamada N, Moritomo Y and Tokura Y 1998 *Phys. Rev. Lett.* **81** 192
[14] Perebinos V and Allen P B 2000 *Phys. Rev. Lett.* **85** 5178
[15] Moreo A, Yunoki S and Dagotto E 1999 *Phys. Rev. Lett.* **83** 2773
[16] Pruschke T, Jarrell M and Freericks J K 1995 *Adv. Phys.* **44** 187
[17] Chung W and Freericks J K 1998 *Phys. Rev.* B **57** 11 955
[18] Chattopadhyay A, Millis A J and Das Sarma S 2000 *Phys. Rev.* B **61** 10 738
[19] Pruschke Th, Cox D L and Jarrell M 1993 *Phys. Rev.* B **47** 3553
[20] Quijada M, Černe J, Simpson J R, Drew H D, Ahn K H, Millis A J, Shreekala R, Ramesh R, Rajeswari M and Venkatesan T 1998 *Phys. Rev.* B **58** 16 093
[21] Kaplan S G, Quijada M, Drew H D, Tanner D B, Xiong G C, Ramesh R, Kwon C and Venkatesan T 1996 *Phys. Rev. Lett.* **77** 2081
[22] Lee H J, Jung J H, Lee Y S, Ahn J S, Noh T W, Kim K H and Cheong S-W 1999 *Phys. Rev.* B **60** 5251
[23] Mahan G D 1990 *Many-particle Physics* 2nd edn (New York: Plenum)
[24] Zhao G-m, Kang D J, Prellier W, Rajeswari M and Keller H 1999 *Preprint* cond-mat/9912355
[25] Ishihara S, Yamanaka M and Nagaosa N 1997 *Phys. Rev.* B **56** 686
[26] Mack F and Horsch P 1999 *Physics of Manganites* ed T A Kaplan and S D Mahanti (New York: Plenum) p 103
[27] Nagaev E L 1970 *Sov. Phys.–Solid State* **11** 2249
[28] Nagaev E L 1998 *Phys. Rev.* B **58** 827
[29] Kubo K and Ohata N 1972 *J. Phys. Soc. Japan* **33** 21
[30] Furukawa N 1999 *Physics of Manganites* ed T A Kaplan and S D Mahanti (New York: Plenum) p 1
[31] Wang X 1998 *Phys. Rev.* B **57** 7427
[32] Alexandrov A S and Mott N F 1994 *Rep. Prog. Phys.* **57** 1197
[33] Martin M C, Shirane G, Endoh Y, Hirota K, Moritomo Y and Tokura Y 1996 *Phys. Rev.* B **53** 14 285
[34] Rushbrooke G S and Wood P J 1958 *Mol. Phys.* **1** 257
[35] Perring T G, Aeppli G, Hayden S M, Carter S A, Remeika J P and Cheong S-W 1996 *Phys. Rev. Lett.* **77** 711
[36] Fernandez-Baca J A, Dai P, Hwang H Y, Kloc C and Cheong S-W 1998 *Phys. Rev. Lett.* **80** 4012
[37] Lynn J W, Erwin R W, Borchers J A, Huang Q, Santoro A, Peng J-L and Li Z Y 1996 *Phys. Rev. Lett.* **76** 4046
[38] Zhao G-m 2000 *Phys. Rev.* B **62** 11 639
[39] Golosov D I 2000 *Phys. Rev. Lett.* **84** 3974
[40] Alexandrov A S and Bratkovsky A M 1999 *J. Phys.: Condens. Matter* **11** L531